SINGLE-PARTICLE DYNAMICS - RF ACCELERATION

B.W. Montague

CERN
Geneva, Switzerland

1. Synchronous Particle

The voltage across the gap of the accelerating cavity can be expressed as

$$V = \hat{V} \sin \int_0^t \omega \, dt' = \hat{V} \sin \phi(t) \tag{1}$$

where $\hat{V}$, ω are slowly-varying functions of t, or constant.

The accelerating frequency ω is an integral multiple h (harmonic number) of the revolution frequency Ω_0 of the synchronous particle

$$\omega = h \, \Omega_0 = \frac{h \, \beta_0 c}{R_0} \tag{2}$$

Here β_0 c is the velocity and R_0 the average orbit radius of the synchronous particle, which experiences a constant RF phase

$$\phi(t) = \phi_0 = \text{const.}$$

The average bending field $\bar{B}_0$ around the synchronous orbit is given by

$$e \, \bar{B}_0 \, R_0 = p_0 = m_0 c (\beta\gamma)_0 \tag{3}$$

During acceleration at constant radius

$$\frac{dp_0}{dt} = e \, R_0 \, \frac{d\bar{B}_0}{dt} \tag{4}$$

In one revolution, period $2\pi/\Omega_0 = 2\pi \, R_0/\beta_0 c = [\Delta t]_1$, there is a momentum increment

$$[\Delta p_0]_1 = e \, R_0 \, \frac{d\bar{B}_0}{dt} \, [\Delta t]_1 = \frac{2\pi \, e \, R_0^2}{\beta_0 c} \, \frac{d\bar{B}_0}{dt} \tag{5}$$

We have also the relativistic kinematic formula

$$\Delta p = m_0 c\ \Delta(\beta\gamma) = \frac{m_0 c}{\beta}\,\Delta\gamma = \frac{\Delta E}{\Omega\ R} \tag{6}$$

which, with (5), gives the energy gain per revolution

$$[\Delta E_0]_1 = m_0 c^2 [\Delta\gamma_0]_1 = c\beta_0 [\Delta p_0]_1 = 2\pi\ e\ R_0^2\ \frac{d\bar{B}_0}{dt} \tag{7}$$

The energy gain in one revolution is also given by

$$[\Delta E_0]_1 = e\ \hat{V}\ \sin\ \phi_0 \tag{8}$$

Note that we assume $[\Delta\gamma_0]_1 << 1$ above, i.e. that

$$e\ \hat{V}\ \sin\ \phi_0 << m_0 c^2.$$

2. Non-Synchronous Particle

We take as reference the synchronous particle and its parameters, working to first order in the deviations given by

$$\Omega = \Omega_0 + \Delta\Omega;\quad \phi = \phi_0 + \Delta\phi;\quad p = p_0 + \Delta p;\quad E = E_0 + \Delta E;\quad \theta = \theta_0 + \Delta\theta;$$

where θ_0 is the azimuthal angle in the machine of the reference particle, measured positive in the direction of motion. Then we have

$$\Delta\phi = -\ h\ \Delta\theta$$

$$\Delta\Omega = \frac{d}{dt}\,(\Delta\theta) = -\,\frac{1}{h}\ \frac{d}{dt}\,(\Delta\phi) = -\,\frac{1}{h}\ \frac{d\phi}{dt} \tag{9}$$

The dispersion in revolution frequency, η, is defined as

$$\eta = -\,\frac{p}{\Omega}\ \frac{d\Omega}{dp} = \alpha - \frac{1}{\gamma^2} \tag{10}$$

where $\alpha = \dfrac{1}{\gamma_t^{\,2}}$ is the momentum compaction factor and γ_t is the transition energy in units of the particle rest energy. With this definition, η is positive above transition energy, $\gamma > \gamma_t$. From (9) and (10) we obtain

$$\Delta p = - \frac{p}{\eta \Omega} \Delta\Omega = \frac{p}{h \eta \Omega} \frac{d\phi}{dt} \tag{11}$$

On each revolution a particle gains an energy

$$[\Delta E]_1 = e \hat{V} \sin \phi \tag{12}$$

which, from (6), corresponds to a momentum increment of

$$[\Delta p]_1 = \frac{[\Delta E]_1}{R \Omega} = \frac{e \hat{V}}{R \Omega} \sin \phi \tag{13}$$

Since the revolution time is $\frac{2\pi}{\Omega}$, the average rate of momentum gain over one revolution is

$$\dot{p} = \left\langle \frac{dp}{dt} \right\rangle = \frac{e \hat{V}}{2\pi R} \sin \phi$$

and so

$$R \dot{p} = \frac{e \hat{V}}{2\pi} \sin \phi \tag{14}$$

For the synchronous particle we subtract

$$R_0 \dot{p}_0 = \frac{e \hat{V}}{2\pi} \sin \phi_0$$

and obtain

$$R \dot{p} - R_0 \dot{p}_0 = \Delta(R \dot{p}) = \frac{e \hat{V}}{2\pi} [\sin \phi - \sin \phi_0] \tag{15}$$

Expanding to first order

$$\begin{aligned} \Delta(R \dot{p}) &= R_0 \Delta\dot{p} + \dot{p}_0 \Delta R + \ldots \\ &= R_0 \Delta\dot{p} + \dot{p}_0 \left[\left(\frac{dR}{dp} \right)_0 \Delta p + \ldots \right] \\ &= R_0 \Delta\dot{p} + \left(\frac{dp}{dt} \frac{dR}{dp} \right)_0 \Delta p + \ldots \\ &= R_0 \Delta\dot{p} + \dot{R}_0 \Delta p \end{aligned}$$

Thus
$$\Delta(R \dot{p}) = \frac{d}{dt} (R_0 \Delta p) = \frac{d}{dt} \left(\frac{\Delta E}{\Omega_0} \right) \tag{16}$$

Equations (15) and (16) combine to give one equation of motion

$$\frac{d}{dt}\left(\frac{\Delta E}{\Omega_0}\right) = \frac{e\ V}{2\pi}\left[\sin\phi - \sin\phi_0\right] \tag{17}$$

The other equation of motion comes from (11) using (6)

$$\frac{d\phi}{dt} = \frac{h\ \eta_0\ \Omega_0}{p_0\ R_0}\left(\frac{\Delta E}{\Omega_0}\right) \tag{18}$$

In (18), η, Ω, p and R have been evaluated for the synchronous particle, which is permissible since we are working only to first order. Also, for the moment, we consider p_0 to be constant in time, which is valid for storage rings or for accelerators over a limited range of energy.

The two first-order differential equations (17) and (18) can be combined into one second-order equation

$$\frac{d}{dt}\left[\frac{p_0\ R_0}{h\ \eta_0\ \Omega_0}\ \frac{d\phi}{dt}\right] - \frac{e\ \hat{V}}{2\pi}\left[\sin\phi - \sin\phi_0\right] = 0 \tag{19}$$

Replacing ϕ by $\phi_0 + \Delta\phi$, approximating for $\Delta\phi \ll 1$ and for constant coefficients, yields the simplified linearised equation of small-amplitude synchrotron oscillation

$$\frac{d^2}{dt^2}(\Delta\phi) - \frac{e\ \hat{V}\ h\ \eta_0\ \Omega_0\ \cos\phi_0}{2\pi\ p_0\ R_0}(\Delta\phi) = 0 \tag{20}$$

3. Phase Stability

Equation (20) has stable oscillatory solutions if $\eta_0 \cos\phi_0 < 0$. The frequency of small-amplitude synchrotron (or energy) oscillations is then given by

$$\Omega_s = \left[-\frac{e\ \hat{V}\ h\ \eta_0\ \Omega_0\ \cos\phi_0}{2\pi\ p_0\ R_0}\right]^{\frac{1}{2}} \tag{21}$$

Below transition energy, i.e. for $\gamma < \gamma_t$, one sees from (10) that $\eta_0 < 0$, consequently $\cos\phi_0 > 0$ and either

$$\text{(a)} \quad 0 < \phi_0 < \frac{\pi}{2} \rightarrow \sin\phi_0 > 0$$

or

$$\text{(b)} \quad \frac{3\pi}{2} < \phi_0 < 2\pi \rightarrow \sin\phi_0 < 0$$

It follows from (12) that (a) corresponds to acceleration and (b) to deceleration of the particles. Above transition energy $\eta > 0$, $\cos \phi_0 < 0$ and stability requires either

$$\text{(c)} \quad \frac{\pi}{2} < \phi_0 < \pi \rightarrow \sin \phi_0 > 0 \quad \text{(acceleration)}$$

or

$$\text{(d)} \quad \pi < \phi_0 < \frac{3\pi}{2} \rightarrow \sin \phi_0 < 0 \quad \text{(deceleration)}$$

At transition energy η_0 vanishes, Ω_s goes to zero and there is no phase stability. During acceleration through transition energy in a proton synchrotron, the RF phase must be switched abruptly from ϕ_0 to $\pi - \phi_0$ in order to maintain stability above transition. In a real beam with a non-zero energy spread the timing of the phase switching cannot be accurate for all particles, and some "blow-up" in phase space is unavoidable. This is enhanced by space-charge forces, and various methods such as multiple phase-switching and the γ_t - jump have been used to minimise the ill effects.

4. Hamiltonian for Synchrotron Oscillations

We now introduce the "energy" variable W canonically conjugate to the "position" variable ϕ;

$$W = \frac{\Delta E}{\Omega_0} \tag{22}$$

which has the dimensions of action (energy times time). Then the equations of motion (17) and (18) can be derived from the Hamiltonian

$$H(\phi, W) = \frac{h\ \eta_0\ \Omega_0}{2p_0\ R_0} W^2 + \frac{e\ \hat{V}}{2\pi} [\cos \phi - \cos \phi_0 + (\phi - \phi_0)\sin \phi_0] \tag{23}$$

using the formal rules

$$\dot{\phi} = \frac{d\phi}{dt} = \frac{\partial H}{\partial W} = \frac{h\ \eta_0\ \Omega_0}{p_0\ R_0}\ W \tag{24}$$

$$\dot{W} = \frac{dW}{dt} = -\frac{\partial H}{\partial \phi} = \frac{e\ \hat{V}}{2\pi} [\sin \phi - \sin \phi_0] \tag{25}$$

The parameters η_0, Ω_0, ϕ_0, p_0, R_0 and $\hat{V}$ can vary with time and the Hamiltonian is therefore, in general, time-dependent. However, in most cases the variation is slow enough that it can be neglected for the dis-

cussion of synchrotron motion over a few periods of oscillation, in which case

$$\frac{dH}{dt} = \frac{\partial H}{\partial t} \approx 0$$

For this to be valid, the fractional change in synchrotron frequency during one radian of oscillation must be small, a condition expressed by the dimensionless adiabaticity parameter

$$\varepsilon = \frac{1}{\Omega_s^2} \frac{d\Omega_s}{dt} << 1 \qquad (26)$$

During acceleration in a synchrotron at constant $\hat{V}$, ϕ_0, the main variation arises from $p_0(t)$, and condition (26) can be written, using (14) and (21), as

$$\left[- \frac{e \hat{V} \sin \phi_0 \tan \phi_0}{2\pi h \eta_0 p_0 \beta c} \right]^{\frac{1}{2}} << 1 \qquad (27)$$

which is usually well satisfied except in the immediate vicinity of transition energy, where η_0 becomes very small.

The motion of particles is conveniently represented by their trajectories in the (ϕ, W) phase plane; these trajectories are contours of constant Hamiltonian, Eq. (23). Families of such curves are shown in Fig. 1 for $\gamma > \gamma_t$ ($\eta_0 > 0$) and for three values of stable phase angle ϕ_0. For a machine with harmonic number h the pattern repeats h times along the ϕ axis.

Particles move in time along the trajectories, in the direction of the arrows, according to Eqs. (24) and (25). In each interval of 2π are two fixed points where $\dot{\phi} = \dot{W} = 0$. The stable fixed point at $\phi = \phi_0$, W = 0, corresponding to the synchronous particle, lies inside the stable region (or "bucket") bounded by the separatrix. The unstable fixed point is at $\phi_u = \pi - \phi_0$, W = 0, at the extreme limit of the separatrix; the motion of particles becomes infinitely slow as they approach this point.

The case of $\phi_0 = \pi$ corresponds to zero acceleration, $\dot{p}_0 \equiv 0$, or "stationary buckets". The separatrix extends between adjacent unstable fixed points, and trajectories outside the stable region do not cross between the upper and lower half planes. For $\phi_0 \neq \pi$, corresponding to acceleration, the separatrix is bounded by only one unstable fixed point and particles can cross between upper and lower half planes outside the stable regions.

The examples of Fig. 1 have been drawn for $\frac{\pi}{2} < \phi_0 \leq \pi$, corresponding to $\eta_0 > 0$ and $\sin \phi_0 \geq 0$ (acceleration for $\phi_0 < \pi$). The trajectory patterns for $\eta_0 < 0$ and $\sin \phi_0 < 0$ (deceleration) are obtained from Fig. 1 by reflection symmetries in the $W = 0$ and $\phi = \pi$ axes and displacements along ϕ, according to the scheme of Fig. 2.

5. Oscillation Amplitudes

For a particle inside the stable region the limits of oscillation amplitude in W are given by $\dot{W} = 0$, for which Eq. (25) gives the two solutions

$$\phi = \phi_0$$

and

$$\phi = \pi - \phi_0 = \phi_u$$

this second solution corresponding to the unstable fixed point. The first solution substituted into (23) gives the value of the Hamiltonian for the trajectory having extrema $\hat{W}$ in amplitude, and we can write

$$H(\phi, W) = \frac{h\,\eta_0\,\Omega_0}{2p_0\,R_0}\,\hat{W}^2 = \frac{h\,\eta_0\,\Omega_0}{2p_0\,R_0}\,W^2 + \frac{e\,\hat{V}}{2\pi}\,[\cos\phi - \cos\phi_0 + (\phi - \phi_0)\sin\phi_0] \quad (28)$$

From Eq. (24) the extrema in phase are given by $W = 0$, which in (28) leads in general to a transcendental equation to obtain $\phi(\hat{W})$. Two special cases are of interest.

For stationary buckets, $\eta_0 < 0$, $\phi_0 = 0$, putting $W = 0$ in (28) yields

$$\begin{aligned} \frac{h\,\eta_0\,\Omega_0\,\hat{W}^2}{2p_0\,R_0} &= \frac{e\,\hat{V}}{2\pi}\,[\cos\phi - 1] \\ &= -\frac{e\,\hat{V}}{\pi}\sin^2\left(\frac{\phi}{2}\right) \end{aligned} \quad (29)$$

This is of identical form to the pendulum equation discussed in Lecture 3, and gives the limits of oscillation amplitude in phase

$$\phi_\ell = \pm\, 2\arcsin\left[\frac{\pi\,h(-\eta_0)\Omega_0\,\hat{W}^2}{2e\,\hat{V}\,p_0\,R_0}\right]^{\frac{1}{2}} \quad (30)$$

A similar result can be obtained when $\eta_0 > 0$.

For non-stationary buckets an approximate relation can be obtained for small oscillation amplitudes by putting

$$\Delta\phi = \phi - \phi_0 << 1$$

and expanding

$$\cos\phi - \cos\phi_0 + (\phi - \phi_0)\sin\phi_0 = \cos(\phi_0 + \Delta\phi) - \cos\phi_0 + \Delta\phi \sin\phi_0$$

$$\approx - \frac{(\Delta\phi)^2}{2} \cos\phi_0 \qquad (31)$$

Using (31) in (28) with W = 0 as before we have

$$\Delta\phi = \pm \left[\frac{- 2\pi h \eta_0 \Omega_0}{e \hat{V} p_0 R_0 \cos\phi_0} \right]^{\frac{1}{2}} \hat{W} \qquad (32)$$

One sees that (30) and (32) are equivalent for small amplitudes.

The ratio $\hat{W}/\Delta\phi$ is an important parameter in matching bunches of particles into RF buckets, for example when transferring a beam from one accelerator into another. Individual particles move on trajectories of constant Hamiltonian, and, to ensure that the shape (or position) of the bunch as a whole does not execute coherent oscillations, the equi-density contours of the bunch must be homothetic with the Hamiltonian trajectories. Bunch matching is achieved in practice by suitable manipulations, abrupt or slow, of the RF voltage $\hat{V}$ and stable phase angle ϕ_0.

6. Limits of Stable Region

We have already seen that the separatrix limiting the stable region terminates at an unstable fixed point W = 0, $\phi_u = \pi - \phi_0$. We can therefore substitute these values in (28) in order to determine the extrema of W corresponding to the separatrix, which is the limiting stable trajectory. Since $\cos(\pi - \phi_0) = - \cos\phi_0$, these extrema $(\hat{W})_{sep}$ are given by

$$\frac{h \eta_0 \Omega_0}{2 p_0 R_0} (\hat{W})^2_{sep} = \frac{e \hat{V}}{2\pi} [- 2\cos\phi_0 + (\pi - 2\phi_0)\sin\phi_0]$$

or

$$(\hat{W})^2_{sep} = \frac{e \hat{V} p_0 R_0}{\pi h \eta_0 \Omega_0} [(\pi - 2\phi_0)\sin\phi_0 - 2\cos\phi_0] \qquad (33)$$

The other extremum of phase ϕ_e is obtained by using (33) in (28) with $W = 0$ as before, and $\phi = \phi_e$. Then

$$\cos \phi_e - \cos \phi_0 + (\phi_e - \phi_0)\sin \phi_0 = (\pi - 2\phi_0)\sin \phi_0 - 2\cos \phi_0$$

whence

$$\cos \phi_e - \phi_e \sin \phi_0 = (\pi - \phi_0)\sin \phi_0 - \cos \phi_0 \qquad (34)$$

This transcendental equation in $\phi_e(\phi_0)$ reduces to $\cos \phi_e = -1, +1$ for $\phi_0 = 0, \pi$, and thus yields the adjacent unstable fixed point, as expected for stationary buckets.

7. Adiabatic Damping

We have so far assumed a constant Hamiltonian on the basis of the condition (26) being fulfilled. This is perfectly satisfactory for discussing the motion on a time scale short compared with that of the variation of parameters such as p_0, η_0, $\hat{V}$, etc. In a synchrotron, however, these parameters can vary over a large range during an acceleration cycle, even though the rate of variation may be slow and will normally satisfy (26). We thus have to study the long-term evolution of the motion under adiabatic changes of the parameters.

Since (ϕ, W) are canonically-conjugate variables, we know that Liouville's theorem holds and that arbitrary areas in the (ϕ, W) phase plane are conserved in a canonical transformation. However, with changing parameters the stable trajectories in the phase plane do not exactly close over one cycle of synchrotron oscillation and it is not then obvious that area conservation can be invoked. One must then apply the adiabatic theorem (also called the Boltzmann-Ehnenfest theorem), which states that if q, p are canonically-conjugate variables of an oscillatory system with slowly changing parameters, then the action integral

$$I = \oint p \, dq = \text{an invariant}$$

where the integral is taken over one period of oscillation. The validity conditions for the adiabatic theorem are discussed by Landau and Lifshitz [1].

Applying this to the small-amplitude synchrotron oscillations we have

$$I = \oint W \, d\phi = \oint W \frac{d\phi}{dt} \, dt = \overline{\left(W \frac{d\phi}{dt} \right)} \frac{2\pi}{\Omega_s} \tag{35}$$

where the integrand is averaged over one period of synchrotron oscillation. Then from (21) and (24) we have

$$I = \frac{h \eta_0 \Omega_0}{p_0 R_0} \overline{W^2} \, 2\pi \left[\frac{-2\pi p_0 R_0}{e \hat{V} h \eta_0 \Omega_0 \cos \phi_0} \right]^{\frac{1}{2}}$$

$$= \overline{W^2} \left[\frac{-(2\pi)^3 h \eta_0 \Omega_0}{p_0 R_0 e \hat{V} \cos \phi_0} \right]^{\frac{1}{2}} = \text{invariant} \tag{36}$$

Since, for sinusoidal oscillations, $\hat{W}^2 = 2\overline{W^2}$, the peak value $\hat{W}$ varies under adiabatic changes of parameters as

$$\hat{W} \propto \left[\frac{-p_0 R_0 \hat{V} \cos \phi_0}{\eta_0 \Omega_0} \right]^{\frac{1}{4}} \tag{37}$$

The adiabatic variation of phase amplitude is obtained similarly, starting from

$$I = \oint \Delta\phi \, dW = \oint \Delta\phi \frac{dW}{dt} \, dt = \overline{\left(\Delta\phi \frac{dW}{dt} \right)} \frac{2\pi}{\Omega_s} \tag{38}$$

Approximating (25) for small amplitudes $\Delta\phi$, with $\phi = \phi_0 + \Delta\phi$, one has

$$\frac{dW}{dt} = \frac{e \hat{V}}{2\pi} [\sin \phi - \sin \phi_0] \approx \frac{e \hat{V}}{2\pi} \cos \phi_0 \, \Delta\phi$$

leading to

$$\Delta\phi \propto \left[\frac{-\eta_0 \Omega_0}{p_0 R_0 \hat{V} \cos \phi_0} \right]^{\frac{1}{4}} \tag{39}$$

From (39) one sees that, during acceleration, p_0 increasing and the other parameters constant, the phase excursion $\Delta\hat{\phi}$ is reduced as the one-fourth power of the momentum. This is loosely called "adiabatic damping" of phase oscillations, although in fact, with (37), it is evident that $\hat{W} \, \Delta\hat{\phi}$ is invariant, Liouville's theorem holds and there is no damping of the area in the phase plane.

8. Nonlinear Motion

So far we have mainly considered the linearised motion appropriate to particles with small oscillation amplitudes. At larger amplitudes the motion becomes appreciably nonlinear and, in particular, the oscillation frequency is reduced, tending towards zero for the limiting trajectory of the separatrix. This frequency cannot be evaluated in closed form, but can be expressed in the form of an integral over ϕ, by replacing W in (23) by $\dot{\phi}$ from (24) and integrating between the limits of ϕ given by the solutions of (28). Curves of the large amplitude synchrotron frequency are given by Bruck [2].

In the case of a mismatched bunch, the amplitude dependence of frequency causes the large amplitude trajectories to lag behind the central motion, thus distorting the original density distribution. After a sufficient time the outer regions are wrapped many times around the centre, a process known as filamentation, and the macroscopic density curves become homothetic with the dynamical trajectories. The apparent bunch area has now been blown up in a non-Liouvillian way although on the microscopic scale Liouville's theorem still holds formally.

The highly nonlinear motion in the neighbourhood of the unstable fixed points is of particular importance for stacking in proton storage rings and will be discussed further in that context.

9. Stacking

RF stacking in longitudinal phase space of a storage ring involves accumulating succesive pulses of protons such that each pulse occupies a slightly different energy range from its neighbours. Because of the tight momentum compaction of AG machines these different energies largely overlap in physical (and betatron) space, where the particle density becomes greatly enhanced as compared with that of a single stacked pulse.

The sequence of stacking operations consists of injecting a beam pulse on to the injection orbit, trapping and matching the bunches into the RF buckets, accelerating out to the stacking orbit and finally turning off the RF, allowing the bunches to debunch. This sequence is repeated a number of times to build up a complete stack. The above steps require fairly complicated manipulations of the RF system parameters.

The detailed behaviour of the particle distribution in the (W, ϕ) phase plane is governed by two basic features. Firstly, as a direct consequence of Liouville's theorem, the phase area transported upwards in energy by an accelerating RF bucket must be accompanied by the downwards transport of an equal phase area in the region outside the bucket, a property known as phase displacement. It is immaterial in this connection whether the phase area contains particles or not. The stacking process is thus equivalent to displacing empty phase space and replacing it by occupied phase space.

The second important feature arises from the presence of the unstable fixed points. Near each such point there is a region in which, for any non-zero rate of change of parameters, the motion is non-adiabatic. The effect of this is similar in character to that of filamentation; although Liouville's theorem holds on a sufficiently microscopic scale there can be an apparent dilution due to the highly nonlinear motion in this region. Clearly, this dilution only occurs if the phase space densities of particles inside and outside the RF bucket are different, for example when the bucket is moving through the edge of the stack.

To illustrate these principles, we first consider the method known as "stacking at the top" or "repetitive stacking", in which each successive pulse is accelerated to the same stacking orbit, i.e. the same "energy", W_t, at which point the RF voltage is abruptly switched off. The motion in the (W, ϕ) phase plane is shown in Fig. 3. At the moment of RF switch-off the bunches appear as in (a), and from Eqs. (24) and (25) one sees that, with $V = 0$, the subsequent evolution is a shearing motion as in (b). Finally, after complete debunching, the energy band around W_t is uniformly populated in ϕ with a density less than that of the original bunches.

On subsequent pulses, assuming the RF buckets fit tightly around the bunches, sparsely populated phase space around W_t is displaced downwards and replaced by denser stuff, tending asymptotically at W_t towards the density of the original bunches. Meanwhile, the more dilute phase space below W_t that is displaced downwards is also being repeatedly traversed by the accelerated buckets and therefore suffers further dilution. After building up a stack of many pulses one might therefore expect a final density distribution in W which has a peak at W_t approaching the original bunch density, and a steady fall-off for lower valves of W. Fig. 4 shows an example of this taken from an experimental result at the ISR.

In another method, called "stacking at the bottom" or "non-repetitive stacking", each successive pulse is deposited at a slightly lower energy than its predecessor. The energy difference ΔW_s between RF switch-off on successive pulses is normally chosen to be approximately the bunch area divided by 2π, i.e. the energy width of an ideal adiabatically debunched pulse. With this method the tail of the stack suffers, on average, less perturbation by the accelerating buckets than for stacking at the top. Consequently, the final density distribution is more uniform, permitting a larger current to be stacked inside a given momentum interval limited by other phenomena. An example is shown in Fig. 5.

In practice one may, for technical or operational reasons, choose one or other method, or even a combination of the two methods to obtain the highest density, for example by starting with stacking at the top and subsequently introducing a step-back on each pulse after the density has built up sufficiently at the top of the stack. Such an example shown in Fig. 6 is typical of present ISR operation.

The overall efficiency of the stacking process is determined by several potentially imperfect mechanisms. Trapping efficiency at injection can in practice be 100% and dilution during the bunch matching can be kept very small. Spill-out of particles from the tightly fitting buckets on entering the stack can be minimised by careful control of RF parameters, taking account of the distortion of the buckets arising from space-charge fields. Longitudinal instabilities can occur during debunching due to the impedance of the vacuum chamber wall; they have the effect of diluting the phase space density of the early pulses stacked but stability is attained once the stack energy spread exceeds a critical value. The various collective effects are covered in the lectures of A. Hofmann.

There remains one fundamental effect which limits the phase space density efficiency which can be achieved, namely the dilution resulting from imperfect adiabaticity near the unstable fixed point during the passage of buckets into the stack. The stacking efficiency η is defined with respect to an idealised stack of n pulses obtained by perfect adiabatic debunching, and is the ratio of the number of particles actually obtained with n pulses inside the ideal momentum width to the number that would have been obtained for the perfect stack.

Because of the nonlinearity and nonadiabaticity, the analytic calculation of η appears to be an intractable problem and computer simulation has been necessary. Early work at MURA [3] led to an empirical formula called Symon's Rule which indicated that the r.m.s. momentum spread δp_{rms} introduced into the edge of a stack by the passage of n buckets is given by

$$\delta p_{rms} = \frac{\sqrt{n}}{2} \Delta p_s$$

where $2\pi \Delta p_s$ is the area of a stationary bucket of the same voltage. Later computer simulation by Swenson [4], Keil and Nakach [5] and Messerschmid [6] has led to an improved empirical rule [7] giving the stacking efficiency as approximately

$$\eta = \frac{1}{\left[1 + \frac{2\Gamma}{3\sqrt{n}\ \alpha(\Gamma)}\right]}$$

where $\Gamma = \sin \phi_0$ is the sine of the stable phase angle for the accelerating bucket and $\alpha(\Gamma)$ is the area ratio of moving to stationary buckets at fixed voltage V. This improved formula agrees quite well with both the computer simulation and the ISR experimental results over a wide range of Γ for n not too small. It corresponds to Symon's rule for $\Gamma \approx 0.5$. For a given n the largest η is obtained for small values of Γ, since $\alpha(\Gamma) \to 1$ for $\Gamma \to 0$. However, for very small values of Γ the stacking time may become unduly long and a compromise must be made with stacking efficiency.

The descriptions above have been somewhat idealised in order to bring out clearly the basic principles. In the absence of detailed analytic theory for the process, efficient stacking in the ISR is achieved by a combination of these basic ideas and a large collection of experimental knowledge. Although the stacking process is rather well understood at the qualitative level, the quantitative behaviour still contains some obscurities.

10. Phase-Displacement Acceleration

In discussing stacking we have seen that the motion of accelerating or decelerating RF buckets displaces an equal area of the surrounding phase space downwards or upwards in energy respectively. This property can be used for accelerating an unbunched stack of particles by repeatedly passing empty RF buckets through the stack from a higher to a lower energy; deceleration can clearly be obtained by the reverse process.

The main advantage of phase-displacement acceleration is the relatively modest size of RF system required. To accelerate large currents, and therefore large phase areas, by the normal method of bunching inside the stable region requires large RF buckets and correspondingly high RF voltages. In contrast, phase-displacement acceleration can be achieved with bucket areas much smaller than the phase space area of the stack, by virtue of the repeated traversals.

This benefit is achieved at the price of a relatively slow rate of acceleration, given by the product of bucket area and the number of buckets per second. Furthermore, the edges of the stack are progressively degraded in density by the repeated passages of the buckets, as in the normal stacking process. The degradation is reduced by using low values of Γ and small buckets, but at the expense of acceleration rate. A further undesirable effect arises from the necessary Q-dependence on momentum; the perturbations produced by the traversing RF buckets sweep particles through nonlinear betatron resonances and considerable care is needed to minimise beam loss and blow-up from this cause. However, this problem could be even more difficult in accelerating large phase space areas inside buckets by the traditional method, and so phase displacement remains an attractive technique in proton storage rings.

REFERENCES

1) L.D. Landau and E.M. Lifshitz; A Course of Theoretical Physics, Vol. 1 Mechanics (2nd ed.), p. 155, Pergamon (1969).

2) H. Bruck; Accélérateurs Circulaires de Particules, Bibliothèque des Sciences et Techniques Nucléaires (1966).

3) K.R. Symon and A.M. Sessler; CERN Symposium 1956, 1, p. 44-58.

4) D.A. Swenson; Int. Conf. on High Energy Acc. 1961 (BNL), p. 187.

5) E. Keil and A. Nakach; Report CERN 66-9 (1966).

6) E.W. Messerschmid; Report CERN-ISR-RF/72-28 (1972).

7) M.J. de Jonge and E.W. Messerschmid; Proc. 1973 Particle Acc. Conf., San Francisco, IEEE Trans. on Nucl. Sci. 20, p. 796 (1973).

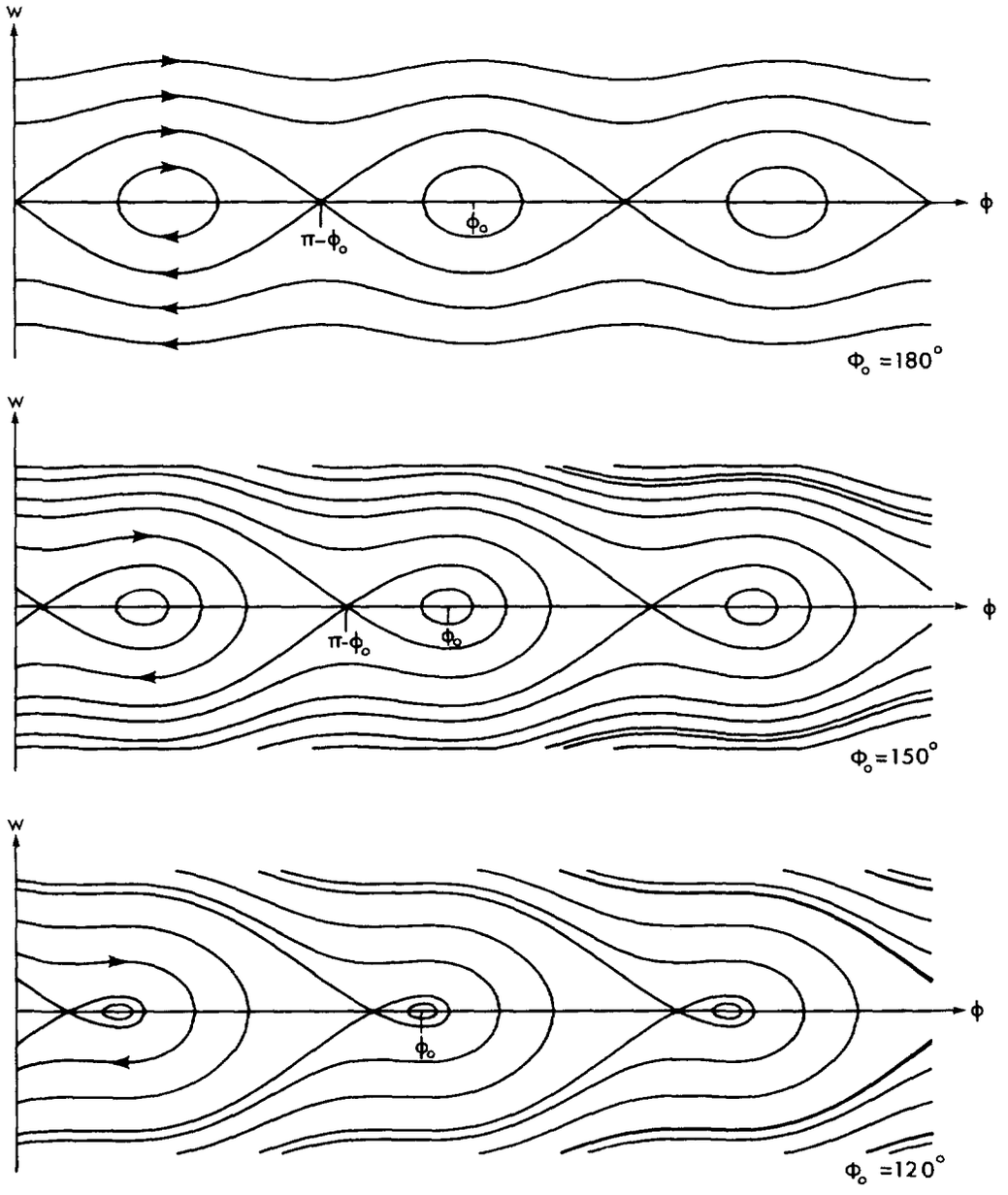

Fig. 1 Trajectories of constant Hamiltonian, $\gamma > \gamma_t$

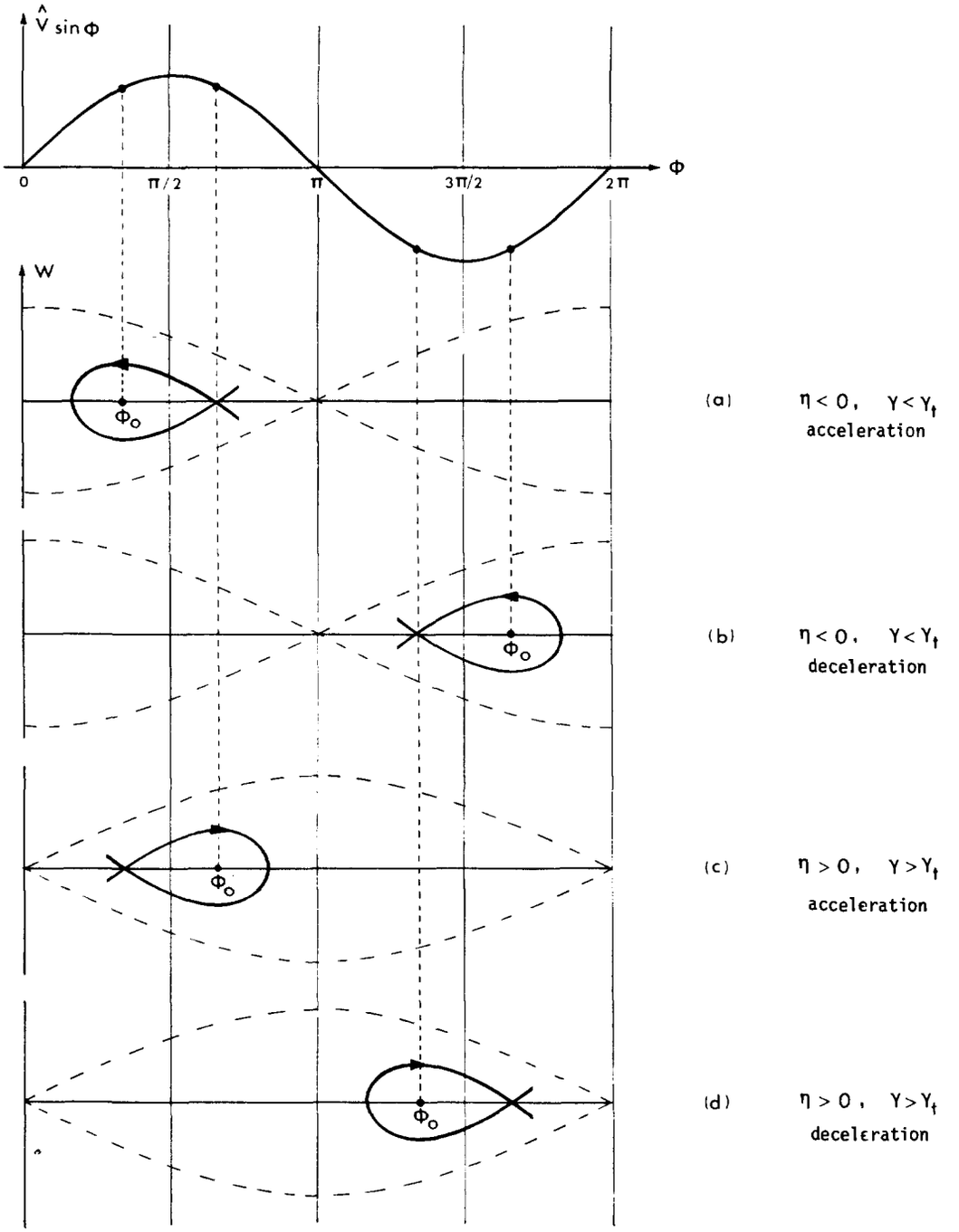

Fig. 2 Phasing of moving and stationary buckets relative to RF voltage

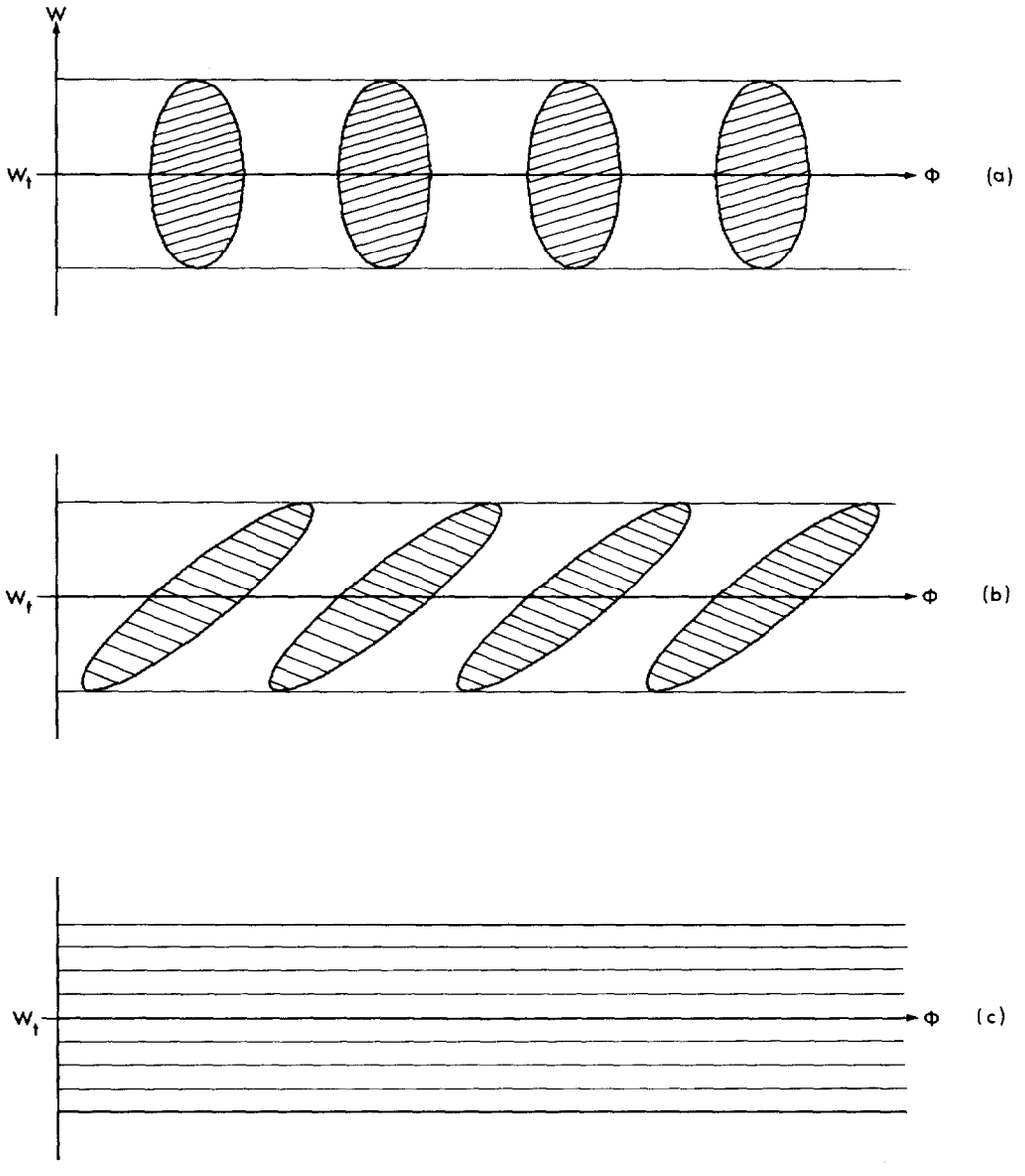

Fig. 3 Debunching and dilution of first pulse in stack

Fig. 4 Density distribution from stacking at the top

Fig. 5 Density distribution from stacking at the bottom

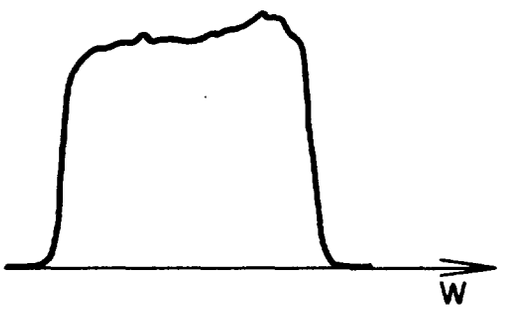

Fig. 6 Density distribution from combined procedure